parison of Theory and Experiment for High-Speed Free-Molecule Flow," Rept. 1032, 1951, NACA.

[6] Laurmann, J. A. and Ipsen, D. C., "Use of a Free Molecule Probe in High Speed Rarefied Gas Flow Studies," TR HE-150-146, April 1957, Univ. of California, Berkeley.

[7] Dewey, C. F., Jr., "Hot Wire Measurements in Low Reynolds Number Hypersonic Flows," *ARS Journal*, Vol. 31, No. 12, Dec. 1961, pp. 1709–1718.

[8] Staylor, W. F. and Morrisette, E. L., "Use of Moderate-Length Hot Wires to Survey a Hypersonic Boundary Layer," *AIAA Journal*, Vol. 5, No. 9, Sept. 1967, pp. 1698–1700.

[9] Laurmann, J. A., "The Free Molecule Probe and Its Use for the Study of Leading Edge Flows," *The Physics of Fluids*, Vol. 1, No. 6, Nov.–Dec. 1958.

[10] Vrebalovich, T., "Heat Loss and Recovery Temperature of Fine Wires in Transonic Transition Flows," *Rarefied Gas Dynamics*, edited by C. L. Brundin, Vol. 2, Academic Press, New York, 1967, pp. 1205–1219.

[11] Schmidt, E. M., "Merged Layer Flow in an Interior Corner," Ph.D. thesis, June 1969, Polytechnic Institute of Brooklyn.

[12] Todisco, A., Pallone, A., and Heron, K., "Hot Wire Measurements of the Stagnation Temperature Field in the Wake of Slender Bodies," RAD-TM 64-32, July 1964, Avco Corp., Wilmington, Mass.

[13] Todisco, A. and Pallone, A., "Near Wake Flow Field Measurements," *AIAA Journal*, Vol. 3, No. 11, Nov. 1965, pp. 2075–2080.

[14] Todisco, A. and Pallone, A., "Measurements in Laminar and Turbulent Near Wakes," AIAA Paper 67-30, New York, 1967.

[15] Rudman, S. and Rubin, S. G., "Hypersonic Flow Over Slender Bodies with Sharp Leading Edges," *AIAA Journal*, Vol. 6, No. 10, Oct. 1968, pp. 1183–1890.

OCTOBER 1971 AIAA JOURNAL VOL. 9, NO. 10

Vortex Computation by the Method of Weighted Residuals Using Exponentials

HARTMUT H. BOSSEL*
University of California, Santa Barbara, Calif.

A method of weighted residuals for the computation of rotationally symmetric quasi-cylindrical viscous incompressible vortex flow is presented. The method approximates the axial velocity and circulation profiles by series of exponentials having $(N+1)$ and N free parameters, respectively. Exponentials are also used as weighting functions. Formal integration results in a set of $(2N+1)$ ordinary differential equations for the free parameters. The governing equations are shown to have an infinite number of discrete singularities. Sample solutions for different swirl parameters and three typical vortex flows (initially uniform axial flow, leading edge vortex, and trailing vortex) are presented, and the effects of external axial velocity and circulation gradients are investigated. The computations point to the controlling influence of the inner core flow on vortex behavior. They also confirm the existence of two particular critical swirl parameter values: S_0, which separates vortex flow which decays smoothly from vortex flows which eventually "breaks down," and S_1, the first singularity of the quasi-cylindrical system, at which point physical vortex breakdown is thought to occur. The results are close to the inviscid values for S_0 and $S_1[(2)^{1/2}$ and $3.8317/2$ for initially uniform axial flow].

I. Introduction

VORTEX flows exist in a bewildering variety of forms and are still only incompletely understood. The study of concentrated vortex flows suffers from a lack of analytical solutions which could serve as guidelines. Perplexing features such as vortex breakdown—the sudden expansion of vortex cores with possible stagnation and flow reversal on the axis appear under certain conditions. Earlier experimental and theoretical work in the area of concentrated vortex flows has been reviewed.[1]

Laminar incompressible steady axisymmetric vortex flows are described by the corresponding form of the Navier-Stokes equations. These equations can be approximated by a parabolic viscous set, analogous to the boundary-layer equations, in regions where the stream surface angle remains small (quasi-cylindrical vortex flow), and by the inviscid equations of rotating flow at and near the axis, and where stream surface angles become large (expansion or contraction of the core).[2]

Some solutions of the inviscid set pertaining to vortex flows at high swirl have been presented[2,3]; here we shall now discuss a method of solving the parabolic viscous set and give corresponding results for different swirl parameters, initial velocity profiles, and external pressure and circulation gradients. Since the regions of validity of the two sets partially overlap on and near the axis, it should be possible to confirm some of the earlier results. The parabolic system has been used before in numerical computations by different methods.[3–6] Gartshore[4] and Mager[6] each used a momentum-integral approach and encountered a singularity which they linked to the vortex breakdown phenomenon and to the critical swirl parameter 3.8317/2 of flow in initially rigid rotation. The present results reinforce this view. Beyond this critical swirl ratio, Refs. 3 and 6 also obtained flows which contrasted in behavior with those below the critical swirl ratio.

The numerical method (N-parameter "exponential series integral method"†) to be used for the present study has pre-

Received August 31, 1970; revision received April 28, 1971. This work was partially supported by NASA Grant NGR 05-010-025.

Index category: Viscous Nonboundary-Layer Flows, Airplane and Component Aerodynamics.

* Associate Professor, Mechanical Engineering Department. Member AIAA.

† The term "integral method" is used here to avoid the cumbersome (but more accurate) terms "method of weighted residuals" or "method of integral relations."

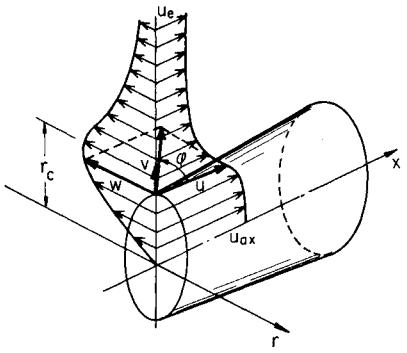

Fig. 1 Coordinate system and velocities.

viously been outlined very briefly in Ref. 7. A related method (N-parameter "power series integral method") has earlier been used successfully to calculate viscous vortex flows.[3,7] The methods were inspired by the success of the Dorodnitsyn method for the calculation of boundary layers,[8,9] especially by its aspects of speed and accuracy. However, the Dorodnitsyn approach with its use of $Y(U)$ in place of $U(Y)$ cannot be directly applied to vortex flows where axial velocity profiles often exhibit overshoot and flow reversal. The present approach circumvents this problem. The soundness of the exponential series integral method has been demonstrated in its application to incompressible and compressible boundary-layer flows.[7,10,11]

There are good reasons for choosing an N-parameter integral method over a finite difference method for a study such as the present one. Many of the open questions in this case only require a qualitative answer, which can be obtained at minimal computing cost by a one or two parameter solution. If accuracy is desired, the number of parameters is increased without any change in the program. Results of the same detail and accuracy as for finite difference methods can then be obtained. The integral approach reduces the solution of partial differential equations to solution of a set of ordinary differential equations. Well-known stable integration schemes, such as the Runge-Kutta method, can be applied. There is little chance of confusing a true singularity of the set of equations to be solved with a singularity of a finite difference scheme replacing it. No iterations are necessary. Finally velocities, stream function, pressure, boundary-layer thickness, shear, etc. can all be computed simply and directly from analytical expressions involving the parameters in the velocity approximation.

The following Sec. II will first describe the computational method. Singularities of the equations are investigated in Sec. III, and a swirl parameter is introduced. Section IV compares results for different orders of approximation and investigates three vortex flows which are of particular interest to the fluid dynamicist: 1) vortex flow with initial uniform axial velocity, 2) vortex flow where the velocity on the axis is initially higher than the freestream velocity (leading edge vortex), and 3) vortex flow where the velocity on the axis is initially lower than the freestream velocity (trailing vortex). Representative velocity profiles and velocity distributions on the axis as a function of distance are given. The effects of positive or negative gradients in the external velocity and circulation distribution are shown. Some conclusions are drawn, and results are summarized in Sec. V.

II. Computational Method

In developing the integral method for a problem in two coordinates, the dependent variables in the partial differential equations are replaced by approximating functions, multiplied by a set of weighting functions, and then formally integrated with respect to one coordinate. There remains a set of ordinary differential equations in the other coordinate for the parameters in the approximating expressions for the dependent variables. The major task in developing the integral method is the correct development of the coefficients in the set of ordinary differential equations—not a difficult task, but one requiring careful bookkeeping. (The FORMAC method has been used in a case of comparable complexity to relegate this task to the computer.[11]) The ordinary differential equations are solved for the parameters by any of a number of standard methods. Knowledge of the parameters at each step permits calculation of the dependent variables and of a number of related variables of interest.

The independent and dependent variables are introduced in Fig. 1. In the following, lower case letters refer to dimensional, upper case letters to nondimensional variables. The indices "∞", "e", "c", and "ax" are used to distinguish conditions in a reference freestream, in the external flow, at a representative constant core radius r_c, and on the axis, respectively.

The dimensional equations for incompressible viscous quasi-cylindrical vortex flow are

$$\frac{\partial u}{\partial x}+\frac{\partial v}{\partial r}+\frac{v}{r}=0$$

$$\frac{w^2}{r}=\frac{1}{\rho}\frac{\partial p}{\partial r} \qquad (1)$$

$$u\frac{\partial u}{\partial x}+v\frac{\partial u}{\partial r}=-\frac{1}{\rho}\frac{\partial p}{\partial x}+\nu\left(\frac{\partial^2 u}{\partial r^2}+\frac{1}{r}\frac{\partial u}{\partial r}\right)$$

$$u\frac{\partial w}{\partial x}+v\frac{\partial w}{\partial r}+\frac{vw}{r}=\nu\left(\frac{\partial^2 w}{\partial r^2}+\frac{1}{r}\frac{\partial w}{\partial r}-\frac{w^2}{r^2}\right)$$

Nondimensional variables are defined as follows:

$$X=x/r_c,\quad Y=R^2/2=Re(r^2/2r_c^2),\quad P=p/(\rho u_\infty^2/2)$$

$$U=u/u_\infty,\quad V=(Re)^{1/2}(v/u_\infty),\quad W=w/u_\infty$$

where the core Reynolds number $Re=u_\infty r_c/\nu$. For convenience we define $H=VR$ and $K=WR$ (circulation). These quantities are introduced into the conservation equations. The pressure P is eliminated by cross-differentiation, and two equations remain for U and K:

$$(\partial/\partial X)(UK)+(\partial/\partial Y)(HK-2Y\partial K/\partial Y+2K)=0$$

$$\partial/\partial X(2Y^2U\partial U/\partial Y+K^2/4)+$$
$$(Y^2\,\partial^2/\partial Y^2)(HU-2Y\partial U/\partial Y)=0$$

where

$$H=-\int_0^Y\frac{\partial U}{\partial X}dY$$

The pressure at any point in the flow is given by

$$P=P_e-\int_Y^\infty\frac{K^2}{4Y^2}dY$$

where

$$P_e=P_0-U_e^2=P_\infty+1-U_e^2$$

The equations are multiplied by weighting functions $g_k(Y)$ and $f_k(Y)$ satisfying $g_k(0), f_k(0)=$ finite, and $g_k(\infty), f_k(\infty)=0$, and are then integrated in the Y-direction:

$$\frac{d}{dX}\int_0^\infty g_kUKdY-\int_0^\infty g_k'HKdY-$$
$$\int_0^\infty(2g_k''Y+4g_k')KdY=0$$

$$\frac{d}{dX}\int_0^\infty(f_k'Y^2+2f_kY)U^2dY-\frac{d}{dx}\int_0^\infty f_k\frac{K^2}{4}dY-$$
$$\int_0^\infty(f_k''Y^2+4Yf_k'+2f_k)HUdY-\int_0^\infty(2f_k'''Y^3+$$
$$14f_k''Y^2+20f_k'Y+4f_k)UdY=0 \qquad (2)$$

The integration is completed with the following choices for

weighting functions and axial velocity and circulation approximations:

$$g_k(Y) = e^{-\sigma_k Y} \quad k = 1,2,\ldots,N$$

$$f_k(Y) = e^{-\sigma_k Y} \quad k = 1,2,\ldots,N+1$$

$$U(X,Y) = (1 - e^{-\alpha Y})\left[U_e(X) + \sum_{n=1}^{N} a_n(X)e^{-n\alpha Y}\right] + U_{ax}(X)e^{-\alpha Y} \quad (3)$$

$$K(X,Y) = W(X,Y)R = (1 - e^{-\alpha Y}) \times \left[K_e(X) + \sum_{n=1}^{N} b_n(X)e^{-n\alpha Y}\right]$$

The external velocity and circulation $U_e(X)$ and $K_e(X)$ are prescribed; the $a_n(X)$, $b_n(X)$ and the velocity on the axis $U_{ax}(X)$ are free parameters. Major reasons for these choices[7] are the exponential character of the flows, ease of analytical integration, and the fact that the approximations satisfy Weierstrass's approximation theorem after a coordinate transformation of the semi-infinite region $0 \leq Y < \infty$ into $1 \geq \eta > 0$, with $\eta = e^{-\alpha Y}$.

Introduction of the approximating expressions and the weighting functions into Eqs. (2) results in the following set of ordinary differential equations for U_{ax} and the parameters $a_n(X)$ and $b_n(X)$:

$$\sum_{n=1}^{N} \dot{a}_n A_{n,k} + \sum_{n=1}^{N} \dot{b}_n B_{n,k} + \dot{U}_{ax} C_k = -\dot{U}_e D_k - \dot{K}_e E_k - F_k \qquad k = 1,2,\ldots,N+1 \quad (4)$$

$$\sum_{n=1}^{N} \dot{a}_n \mathbf{A}_{n,k} + \sum_{n=1}^{N} \dot{b}_n \mathbf{B}_{n,k} + \dot{U}_{ax} \mathbf{C}_k = -\dot{U}_e \mathbf{D}_k - \dot{K}_e \mathbf{E}_k - \mathbf{F}_k \qquad k = 1,2,\ldots,N)$$

The coefficients are given in the Appendix. Only a small part of the coefficient calculation has to be done at each step; the major part is done only once at the beginning of the computation. The system (4) of $(2N + 1)$ first order ordinary differential equations is first solved (by Gaussian elimination) for the derivative vector $(da_n/dX;\ db_n/dX;\ dU_{ax}/dX)$. A standard method of integration then produces the a_n, b_n, and U_{ax} (the Runge-Kutta method has been used in the present work). Axial velocity $U(X,Y)$, circulation $K(X,Y)$ and swirl velocity $W(X,Y)$ follow from relations (3).

Initial profile parameters a_n, b_n, and U_{ax} for the initial axial velocity and circulation profiles (3) are required to start the calculation. In the case of arbitrary profiles, these parameters are obtained as outlined in Ref. 7 or Ref. 10. In the present study, simple exponential profiles have been used throughout, i.e.,

$$U_{\text{initial}}(Y) = U_e(1 - e^{-\alpha Y}) + U_{ax}e^{-\alpha Y}$$

and

$$K_{\text{initial}}(Y) = K_e(1 - e^{-\alpha Y}) \text{ or } K_e(1 - e^{-2\alpha Y})$$

Exponents $\alpha = 1$, and $\sigma_k = k$, $k = 1, 2,\ldots,N + 1$ were used in all of the calculations.

III. Singularities and Critical Swirl Parameters

Equations (4) represent an algebraic system for the axial derivatives $\dot{a}_n$, $\dot{b}_n$, and $\dot{U}_{ax}$. The system becomes singular, and the derivatives infinite, when the system determinant vanishes while the right-hand side remains nonzero. The very special case when the right-hand side vanishes also will not be considered.

Inspection of system (4) and of the coefficients appearing on its left-hand side (see Appendix) reveals that the coefficients of the system determinant are functions only of the a_n, b_n, U_{ax}, U_e, and K_e, i.e., of the local axial velocity and circulation profiles. Study of the system determinant shows further that for a given local axial velocity profile (i.e., given a_n, U_{ax}, U_e) and a given shape of the circulation profile (i.e., b_n), the determinant may assume the value zero for discrete positive values of K_e^2. In particular, for an N-order approximation of $K(Y)$, N discrete singular result for K_e^2. In this argument the particular type of approximating functions (or weighting functions) is inconsequential. Since any continuous function $K(Y)$ [or $U(Y)$] can be represented by an infinite series of linearly independent functions $\varphi(Y)$ forming a complete set, it follows that the system (4), and in consequence the Eqs. (1) for quasi-cylindrical viscous vortex flow have a countably infinite number of discrete singularities at values of K_e^2 which depend on the particular local axial velocity and circulation profiles.

Where singularities occur, all axial derivatives become infinite, and vortex computation using the quasi-cylindrical set (1) cannot proceed. It is stressed that the appearance of singularities is a local and profile-dependent phenomenon. The profile development in turn is dependent on external axial velocity and circulation gradients [whose influence enters the right-hand side of Eq. (4)] and singularities may or may not be encountered in the course of the flow computation, irrespective of the initial flow profiles (see Sec. IV). However, the initial velocity profile combination fixes the "type" of vortex flow once and for all, since the singularities cannot be crossed in the course of the numerical computation, and other 'types" can therefore not be reached.

The singularities are best expressed in terms of a nondimensional swirl parameter S. Various choices are possible. The one chosen here reduces to the swirl parameter $S = W_c/U_{ax}$ for rigid rotation on the axis and makes direct comparison possible with inviscid results. Let

$$S = (dW/dR)_{ax}R_c/U_{ax}$$

R_c is the radius where the swirl velocity W reaches its maximum value. The swirl parameter is thus identical to that of a rigidly rotating slug of fluid of radius R_c and of swirl velocity $W_c = (dW/dR)_{ax}R_c$ at R_c, and constant axial velocity U_{ax}. In particular, conditions on the axis are similar.

Figure 2 presents the first five singularities for the vortex profiles

$$U(Y) = 1 = \text{constant}$$

$$K(Y) = WR = K_e(1 - e^{-Y})$$

as a function of swirl parameter (for these profiles, $S = 0.792$ K_e) and order of approximation used. The singularities were obtained by computing the derivatives $\dot{a}_n$, $\dot{b}_n$, $\dot{U}_{ax}$ over a wide range of K_e. Each additional approximating term accounts for a new singularity, as expected, while the location of previously computed singularities is only slightly affected. In

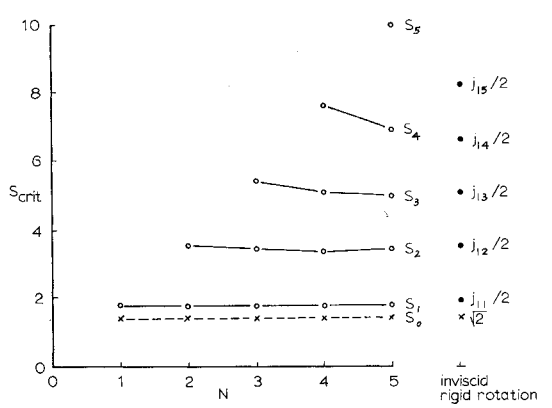

Fig. 2 Singular swirl parameter values for $U(Y) = 1$, and $K(Y) = WR = S(1 - e^{-Y})/0.792$ as a function of order of approximation N.

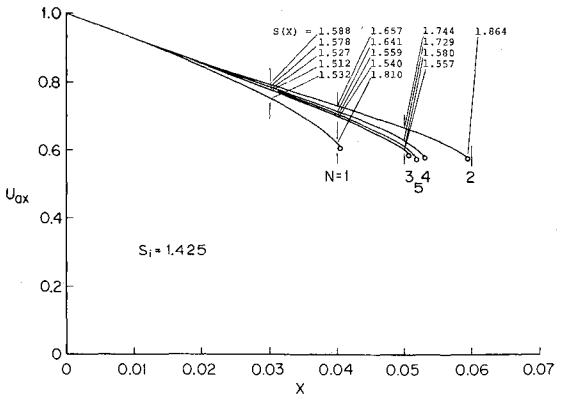

Fig. 3 Development of velocity on the axis as a function of number of parameters used.

particular, the singularity of greatest interest, S_1, remains practically constant. Since there is ample evidence that this first singularity is associated with common physical vortex breakdown, computations failing at singularities, and in particular at S_1, will also be said to "break down" in the following. At each singularity all derivatives jump to infinity in magnitude and reverse signs. Thus contrasting behavior results for flows divided by a singularity. These flows are said to be of different types 1, 2, 3,... in the following. The critical swirl values $j_{1n}/2$ as found from the theory of inviscid rigid rotation[12] are also shown in Fig. 2. (The j_{1n} are the zeros of the Bessel function J_1.)

Figure 2 also gives the swirl parameter S_0 dividing flow which decays smoothly (type 1a) from flow which is abruptly decelerated on the axis and "breaks down" because S_1 is reached (type 1b). The theoretical (inviscid) value[13] for uniform flow in initially rigid rotation is $S_0 = (2)^{1/2}$. The viscous value for S_0 is found from a full vortex computation (see Sec. IVB).

It should be noted again that the critical swirl parameters $S_0, S_1, S_2, \ldots$ are functions of the local profile shape. The example given, which approximates rigid rotation in its inner core, appears to confirm the earlier contention[2,13] that the behavior of viscous vortex flows is governed mainly by inviscid core properties.

IV. Representative Computations

A. Accuracy and Convergence

Results of the present method were compared with previous computations[3] using polynomials in Y in the approximating functions. For $N = 2$ the agreement was within 3% in the velocity profiles.[7] In cases where they can be compared, the computations appear to agree well with those of Hall,[14] who prescribes an outer stream surface shape. Critical runs have been repeated with different orders N of approximation. Figures 3 and 4 show the velocity on the axis and profile development for a breakdown case (type 1b) and $N = 1$–5. There is obvious convergence as N increases. The development of the swirl parameter $S(X)$ is also given in Fig. 3. Cases like these have typical running times on the IBM 360/75 of 5–15 sec for $N = 1$ and 2, and 10–30 sec for $N = 3$–5. All cases discussed below were run with $N = 3$, which appeared to be an efficient compromise between the conflicting demands of high accuracy and low computing time.

B. Initially Uniform Axial Flow

The case where the initial axial velocity profile is uniform while the swirl velocity profile is linear with R in the vicinity of the axis provides a good test of the assertion that vortex behavior is governed by the inviscid properties of the rigidly rotating core. Initial profiles[15] for this case were

$$U(Y) = 1 = \text{constant}$$

$$K(Y) = K_e(1 - e^{-\gamma Y})$$

All computations presented here were obtained for $\gamma = 1$, except where noted. $\gamma = 2$ was used to test scaling effects on the results of the computation. The differences were found to be minimal.

The most important indicator of vortex behavior is a plot of velocity on the axis U_{ax} vs distance X. Figure 5 presents results for different choices of initial swirl parameter S_i. It also gives the swirl parameter $S(X)$ for two neighboring flows of type 1a and 1b. A swirl parameter value of approximately $S_i = 1.4$ separates the smoothly decaying vortex flows (type 1a: $S \lesssim 1.4$) from vortex flows which eventually break down (type 1b: $S_i \gtrsim 1.4$). Note that the theoretical value for the initial swirl value leading to stagnation is $S_i > (2)^{1/2} = 1.41$ for rigid rotation.[13]

Type 1a flow quickly adjusts to an almost constant value of axial velocity and thereafter behaves in a wake-like manner. The swirl parameter $S(X)$ generally decreases. The swirl still counteracts the normal spreading of the wake and the attendant diminishing of the axial velocity deficit; but eventually the axial velocity deficit again decreases, and the axial and swirl velocity profiles decay together.

Flows of type 1b initially behave much like those of type 1a, except that their rate of decrease of U_{ax} is steeper, and the swirl parameter $S(X)$ increases. Eventually the swirl effects overwhelm the restoring tendencies of the wake, the drop of velocity on the axis steepens rapidly, and the computation fails. As an initial swirl parameter value of $S_i \approx 1.8$ is approached, the computation fails increasingly sooner. No solutions can be obtained near this point, whose theoretical value is $S_i = 3.8317/2 = 1.9159$ for rigid rotation.

The velocity profile development for smoothly decaying type 1a flow is shown in Fig. 6. Behavior of type 1b flow is qualitatively similar up to the failure point. The swirl velocity profile shows a gradual decay, while the effect on the axial velocity profile (axial velocity retardation on and near the axis) is more pronounced and increases with swirl.

Figures 7–9 show the development of velocity profiles ($\gamma = 2$) when the initial swirl parameter S_i exceeds S_1. These three cases of types 2, 3, 4 are representative of families of solutions between singularities S_1 and S_4. These solutions develop a multilayer structure, and the core flow reacts differently in each family (i.e., acceleration or deceleration on the axis). All of these cases eventually fail.

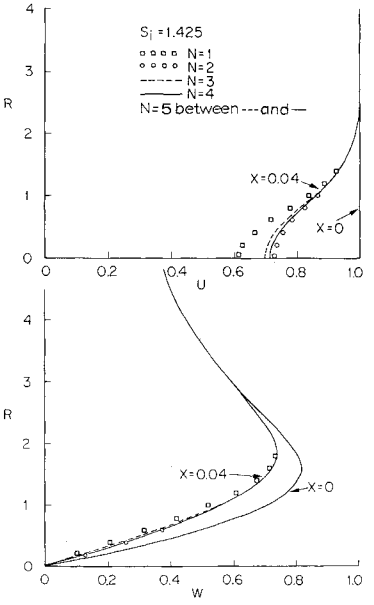

Fig. 4 Velocity profile development as a function of number of parameters used.

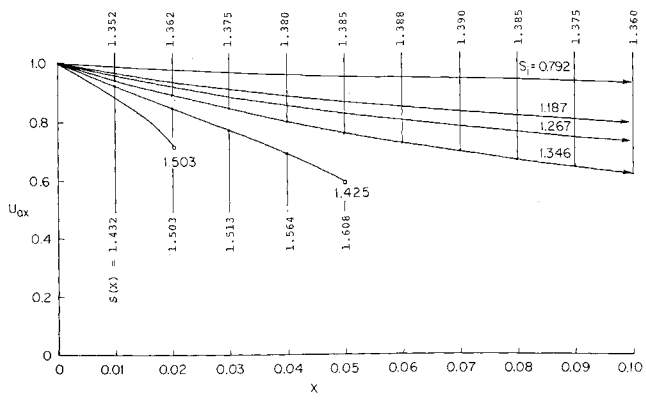

Fig. 5 Development of velocity on the axis as a function of initial swirl. Initially uniform axial flow. Open circles denote failure of the computation.

C. Leading Edge Vortex

Leading edge vortices (as generated at the leading edges of delta wings, for example) are distinguished by axial velocities in the core which exceed the freestream velocity. Initial profiles were chosen as follows:

$$U_{\text{initial}}(Y) = (1 - e^{-Y}) + 2e^{-Y} = 1 + e^{-Y}$$

$$K_{\text{initial}}(Y) = K_e(1 - e^{-Y})$$

This choice is not too good an approximation to the experimental and theoretical profiles,[16,17] but it should serve to demonstrate the effect of higher axial core velocity.

The development of the velocity on the axis for different initial swirl parameters S_i is given in Fig. 10. The swirl parameter $S(X)$ is also shown for two neighboring flows of type 1a and 1b. The behavior is qualitatively again the same as for the vortex with initially uniform axial velocity. A swirl parameter value of $S_i = 1.1$ divides the smoothly decaying type 1a from the breakdown type 1b. This value of S_i is somewhat lower than the theoretical value $S_1 = (2)^{1/2}$ and appears to reflect the influence of the profile shape. One would expect that the regions adjacent to the axis, where the axial velocity is higher, would have some effect on the flow behavior and would therefore tend to bring down the critical value of S_i.

Figure 11 shows the development of the axial and swirl velocity profiles for a (breakdown) type 1b flow. Again there is a strong retarding effect on the axial velocity on and near the axis, while the swirl velocity profile is not greatly affected

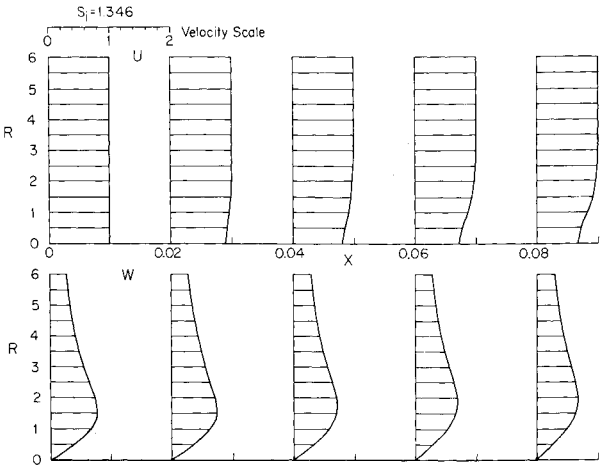

Fig. 6 Velocity profile development for initially uniform axial flow, type 1a.

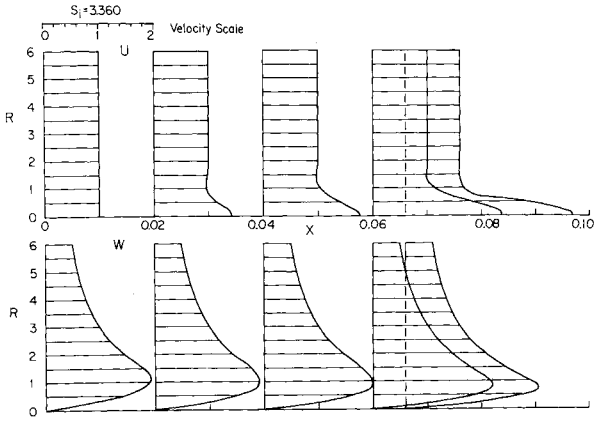

Fig. 7 Velocity profile development for initially uniform axial flow, type 2.

D. Trailing Vortex

The trailing vortex, as generated at the tips of a straight wing, has a wake-like axial velocity distribution with a core velocity smaller than the freestream velocity.[18,19] This velocity retardation near the axis can be expected to lead to earlier vortex stagnation and breakdown.

The initial profiles used were

$$U_{\text{initial}}(Y) = (1 - e^{-Y}) + e^{-Y}/2 = 1 - e^{-Y}/2$$

$$K_{\text{initial}}(Y) = K_e(1 - e^{-Y})$$

This choice appears to come fairly close to actual trailing vortex flows.[18]

The development of velocity on the axis for different initial swirl parameters S_i is plotted in Fig. 12. The swirl parameter $S(X)$ is also given for two neighboring flows of type 1a and 1b. The dividing value S_0 of the initial swirl parameter is now greater than $(2)^{1/2}$, reflecting again the influence of the nonuniform initial axial velocity profile. Figure 13 presents the development of axial and swirl velocity profiles for smoothly decaying type 1a flow.

E. Effects of External Velocity and Circulation Distribution

The strong effects of external axial pressure gradients on vortex flows are well established experimentally,[1,20,21] and in numerical computations.[6,14] A positive external velocity gradient has an accelerating effect on the axial velocity on and near the axis in type 1 vortex flows thus decreasing the local swirl parameter and delaying or preventing breakdown. The effects of circulation gradient are less obvious. Combined external axial velocity and circulation effects may reinforce or cancel each other, depending on sign and magnitude of each and on the type of vortex flow.

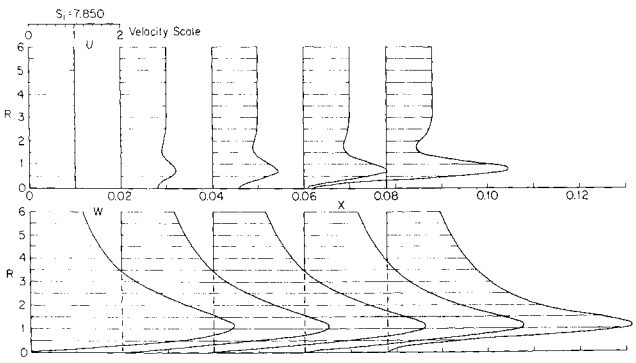

Fig. 8 Velocity profile development for initially uniform axial flow, type 3.

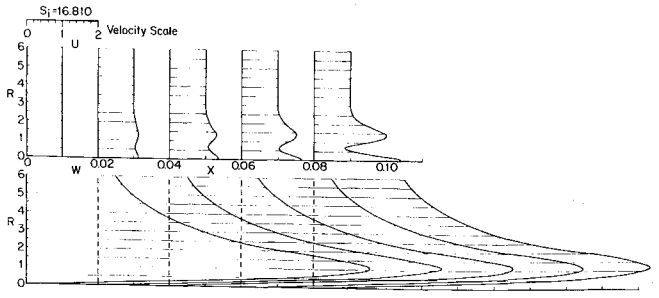

Fig. 9 Velocity profile development for initially uniform axial flow, type 4.

The behavior of vortex flows under external velocity and circulation gradients is of considerable interest in cases where breakdown of vortex flows is to be prevented or induced. Computation by methods such as the present one can indicate what velocity and circulation gradients should be applied and where. The results presented here are for type 1 vortex flows with initially uniform axial velocity. Other initial axial velocity distributions give qualitatively the same result.

Figure 14 presents the results of application of various positive and negative external axial velocity gradients to a type 1b vortex flow of fixed initial swirl and with initially uniform axial velocity. This particular flow breaks down under zero external velocity gradient. The experimental observations (breakdown delay or avoidance through a positive external axial velocity gradient) are confirmed, and the figure also illustrates the significant effect which even very small external velocity gradients can have on the velocity on the axis. Negative velocity gradients lower the critical swirl value and cause type 1b flow to break down sooner. Note that a positive velocity gradient can prevent breakdown and convert a flow from type 1b to 1a, even though the initial profile alone would indicate breakdown in a zero velocity gradient.

Figure 15 presents results of application of different circulation gradients to a type 1a vortex. The effect of a moderate positive circulation gradient is qualitatively the same as for a positive velocity gradient. However, the effect reverses in type 1b flow. Here a positive external circulation gradient results in earlier failure while a negative gradient may prevent failure altogether.

V. Conclusions

An integral method for the computation of viscous incompressible quasi-cylindrical axisymmetric steady vortex flow has been presented. The method uses exponentials in both the approximating expressions for axial velocity and circulation, and as weighting functions. The method is formulated for arbitrary N and can produce quick qualitative studies for

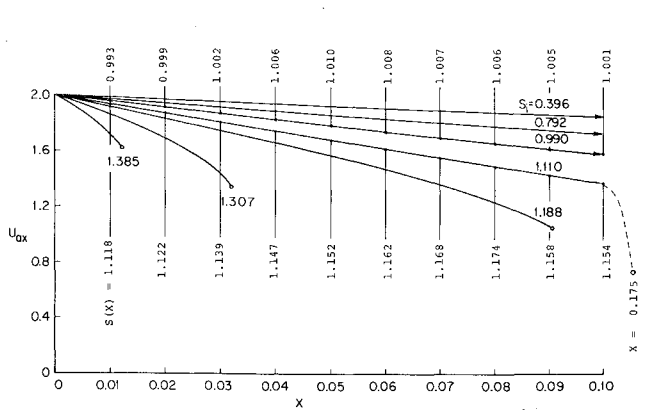

Fig. 10 Development of velocity on the axis as a function of initial swirl; initial flow of leading edge vortex type.

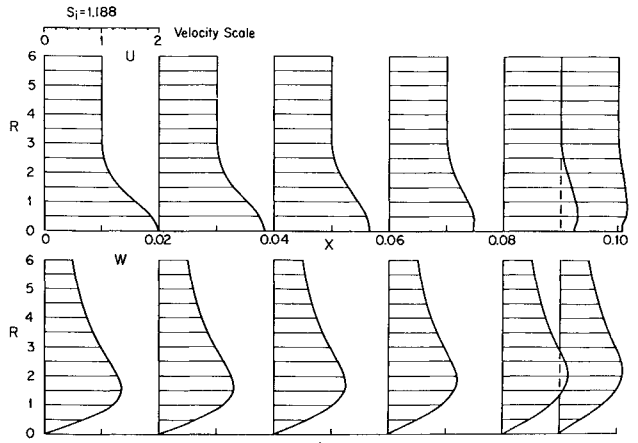

Fig. 11 Velocity profile development for initial flow of leading edge vortex type, type 1b.

$N = 1$ or 2, or more accurate results for $N > 2$. The results presented were for $N = 3$. Computation of a multitude of vortex flows has been efficient and virtually trouble-free. In exploratory investigations such as this one and in more detailed analyses of flows, the use of N-parameter integral methods appears to have distinct advantages and much potential.

Major results of the investigation were as follows:

1) The equations of viscous quasi-cylindrical incompressible vortex flow have an infinite number of discrete singularities. These singularities are best categorized in terms of the swirl parameter of an equivalent cylinder of fluid in rigid rotation. For given vortex velocity profiles the singular swirl parameter values can be computed to determine flow behavior, or results such as the present can be used as guidelines.

2) The singular swirl parameters $S_1, S_2, \ldots$ appear to correspond to the critical values $j_{1n}/2$ of the swirl parameter in the solution of the equation of inviscid flow with initial rigid rotation. (The regions of validity of the viscous and inviscid sets overlap at and near the axis, but the viscous quasi-cylindrical set becomes invalid where stream surfaces expand or contract rapidly.) The exact values of $S_1, S_2, \ldots$ are profile-dependent.

3) At each singularity, all derivatives become infinite in magnitude, and reverse their signs. The result is contrasting behavior of vortex flows on both sides of the singularity. In particular, as the first singularity S_1 is crossed from below (increasing swirl parameter), the tendency to deceleration of the velocity on the axis (and expansion of stream surfaces) changes to one of acceleration (and contraction).

4) For swirl parameters less than a dividing value $S_0 < S_1$ vortex flows show smooth viscous decay of all velocity profiles to the surrounding freestream velocity (type 1a). For swirl

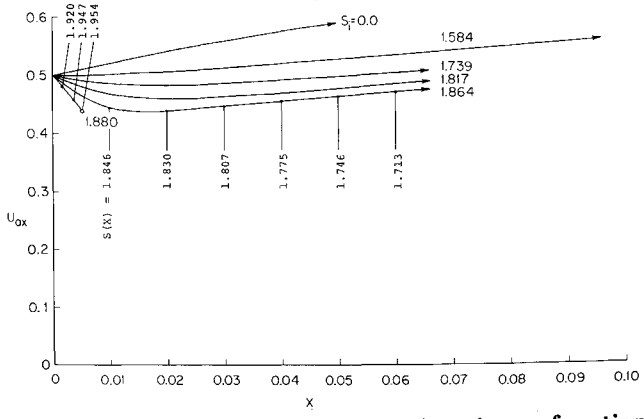

Fig. 12 Development of velocity on the axis as a function of initial swirl; initial flow of trailing vortex type.

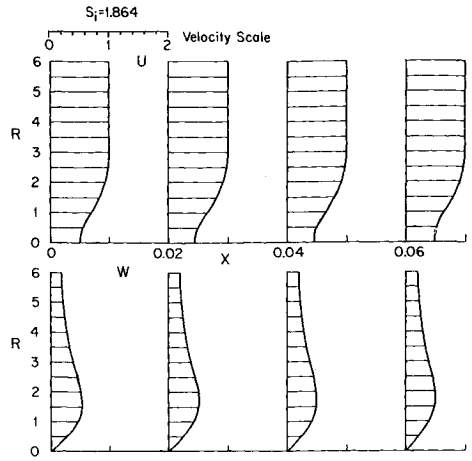

Fig. 13 Velocity profile development for initial flow of trailing vortex type, type 1a.

parameters greater than S_0, increasingly rapid deceleration on the axis develops, the swirl parameter $S(X)$ increases further, and the computation fails when the singularity $S(X) = S_1$ is reached (type 1b). S_0 is profile-dependent, and appears to correspond to the dividing value $S_0 = (2)^{1/2}$ for inviscid flow in initially rigid rotation.

5) External gradients of axial velocity or circulation can affect the swirl parameter $S(X)$ and corresponding flow behavior by either speeding the approach to a singularity, or by avoiding it altogether. In particular, breakdown-prone flows of type 1b with $S(X) > S_0$ can be transformed to type 1a which will not break down. At the dividing point S_0, the effect of an external circulation gradient reverses.

6) Each new singularity first enters at the axis and spreads outward as S is increased. This leads to alternately decelerating and accelerating layers in the axial flow profiles. Thus for $S_3 < S < S_4$ (type 4 flow) four layers exist: a) accelerating core-flow, b) adjacent decelerating layer, c) an accelerating layer, and d) decelerating outer layer. It does not appear that breakdown-stable vortex configurations are possible under these conditions for $S > S_0$, unless external axial velocity and circulation gradients are applied.

7) The singularities are coupled with explosive expansion or implosive contraction of the stream surfaces, and the parabolic viscous subset of the Navier-Stokes equations used in the present work becomes invalid and should be replaced by the inviscid equations of rotating flow, or the full Navier-Stokes equations very close to, and at the singularities.[2] These sets permit continuous solutions for all S, but the possibility of finite transition also exists.[22] The results presented here are valid almost to the point of computational failure in most cases, since stream surface angles remain of the order of a few degrees for typical core Reynolds numbers of order 10^4.

8) No qualitative difference exists in the behavior of flows of same type, but having different velocity profiles (i.e., uniform initial axial flow, leading edge vortex, trailing vortex).

Appendix: Coefficients in the Ordinary Differential Eqs. (4)

$$A_{n,k} = \sum_{l=1}^{N} a_l S_1 + U_e S_2 + U_{ax} S_3$$

$$B_{n,k} = \sum_{l=1}^{N} b_l Q_{1,1}/2 + K_e Q_{1,2}/2$$

$$C_k = \sum_{l=1}^{N} a_l S_7 + U_e S_8 + U_{ax} S_9$$

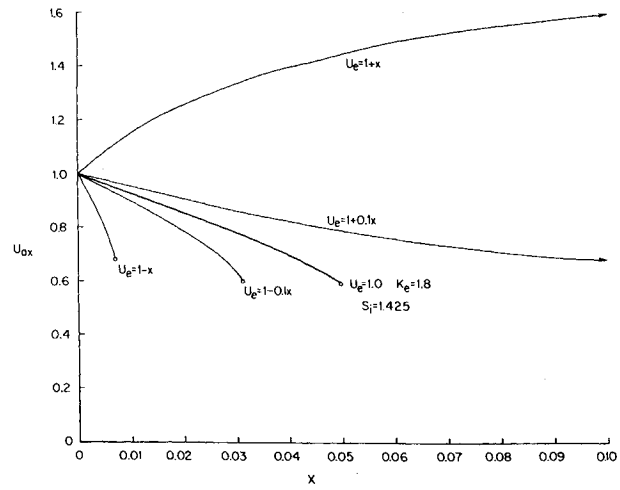

Fig. 14 Development of velocity on the axis as a function of external axial velocity gradient; initially uniform axial flow of type 1b.

$$D_k = \sum_{l=1}^{N} a_l S_4 + U_e S_5 + U_{ax} S_6$$

$$E_k = \sum_{l=1}^{N} b_l Q_{1,4}/2 + K_e Q_{1,5}/2$$

$$F_k = \sum_{n=1}^{N} a_n T_1 + U_e T_2 + U_{ax} T_3$$

$$\mathbf{A}_{n,k} = \sum_{l=1}^{N} b_l \mathbf{S}_1 + K_e \mathbf{S}_2$$

$$\mathbf{B}_{n,k} = \sum_{l=1}^{N} a_l Q_{1,1} + U_e Q_{1,2} + U_{ax} Q_{1,3}$$

$$\mathbf{C}_k = \sum_{l=1}^{N} b_l \mathbf{S}_7 + K_e \mathbf{S}_8$$

$$\mathbf{D}_k = \sum_{l=1}^{N} b_l \mathbf{S}_4 + K_e \mathbf{S}_5$$

$$\mathbf{E}_k = \sum_{l=1}^{N} a_l Q_{1,4} + U_e Q_{1,5} + U_{ax} Q_{1,6}$$

$$\mathbf{F}_k = \sum_{n=1}^{N} b_n \mathbf{T}_1 + K_e \mathbf{T}_2$$

These coefficients involve present values of the parameters a_n, b_n, and of U_{ax}, U_e, and K_e. They must therefore be calcu-

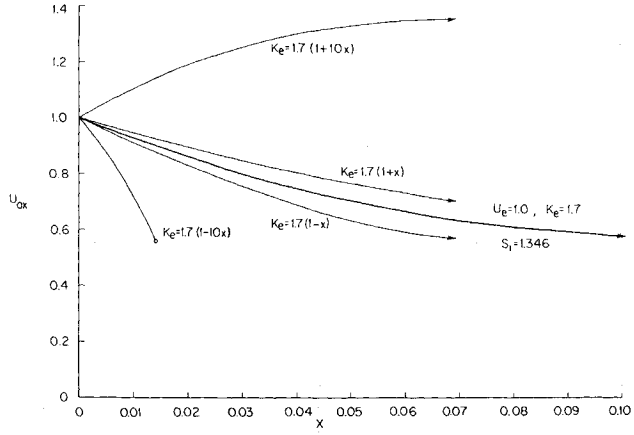

Fig. 15 Development of velocity on the axis as a function of external circulation gradient; initially uniform axial flow of type 1a.

lated anew at each step. However, the numbers Q, S, T, $\mathbf{S}$, and $\mathbf{T}$ are constants which are determined only once at the beginning of the computation. It is convenient to define them in terms of other constants Z, P, and R. The following numbers are all for given l and n. The index k runs from 1 to $N + 1$.

Let

$$
\begin{aligned}
Z_{1,1} &= \sigma_k^{-1} \\
Z_{2,1} &= (\sigma_k + \alpha)^{-1} \\
Z_{3,1} &= (\sigma_k + 2\alpha)^{-1} \\
Z_{4,1} &= (\sigma_k + n\alpha)^{-1} \\
Z_{5,1} &= [\sigma_k + (n+1)\alpha]^{-1} \\
Z_{6,1} &= [\sigma_k + (n+2)\alpha]^{-1} \\
Z_{7,1} &= [\sigma_k + (n+l)\alpha]^{-1} \\
Z_{8,1} &= [\sigma_k + (n+l+1)\alpha]^{-1} \\
Z_{9,1} &= [\sigma_k + (n+l+2)\alpha]^{-1} \\
Z_{10,1} &= [\sigma_k + l\alpha]^{-1} \\
Z_{11,1} &= [\sigma_k + (l+1)\alpha]^{-1} \\
Z_{12,1} &= [\sigma_k + (l+2)\alpha]^{-1} \\
\left.\begin{aligned} Z_{i,2} &= Z_{i,1}Z_{i,1} \\ Z_{i,3} &= 2Z_{i,2}Z_{i,1} \\ Z_{i,4} &= 3Z_{i,3}Z_{i,1} \end{aligned}\right\} & i = 1,2,\ldots,12
\end{aligned}
$$

Then

$$
\left.\begin{aligned} P_{m,1} &= Z_{4,m} - Z_{5,m} \\ P_{m,2} &= Z_{1,m} - Z_{2,m} \\ P_{m,3} &= Z_{2,m} \end{aligned}\right\} m = 1,2,3,4
$$

For the Q's and R's the index $m = 1, 2, 3$:

$$
\begin{aligned}
Q_{m,1} &= Z_{7,m} - 2Z_{8,m} + Z_{9,m} \\
Q_{m,2} &= Z_{4,m} - 2Z_{5,m} + Z_{6,m} \\
Q_{m,3} &= Z_{5,m} - Z_{6,m} \\
Q_{m,4} &= Z_{10,m} - Z_{11,m} \\
Q_{m,5} &= Z_{1,m} - 2Z_{2,m} + Z_{3,m} \\
Q_{m,6} &= Z_{2,m} - Z_{3,m} \\
Q_{m,7} &= Z_{11,m} - Z_{12,m} \\
Q_{m,8} &= Z_{2,m} - Z_{3,m} \\
Q_{m,9} &= Z_{3,m} \\
R_{m,1} &= (Z_{10,m} - Z_{8,m} - Z_{11,m} + Z_{9,m})/[(n+1)\alpha] + \\
&\qquad (-Z_{10,m} + Z_{7,m} + Z_{11,m} - Z_{8,m})/(n\alpha) \\
R_{m,2} &= (Z_{1,m} - Z_{5,m} - Z_{2,m} + Z_{6,m})/[(n+1)\alpha] + \\
&\qquad (-Z_{1,m} + Z_{4,m} + Z_{2,m} - Z_{5,m})/(n\alpha) \\
R_{m,3} &= (Z_{2,m} - Z_{6,m})/[(n+1)\alpha] + (-Z_{2,m} + Z_{5,m})/(n\alpha) \\
R_{m,4} &= (Z_{10,m} - 2Z_{11,m} + Z_{12,m})/\alpha - Z_{10,m+1} + Z_{11,m+1} \\
R_{m,5} &= (Z_{1,m} - 2Z_{2,m} + Z_{3,m})/\alpha - Z_{1,m+1} + Z_{2,m+1} \\
R_{m,6} &= (Z_{2,m} - Z_{3,m})/\alpha - Z_{2,m+1} \\
R_{m,7} &= (-Z_{10,m} + 2Z_{11,m} - Z_{12,m})/\alpha \\
R_{m,8} &= (-Z_{1,m} + 2Z_{2,m} - Z_{3,m})/\alpha \\
R_{m,9} &= (Z_{3,m} - Z_{2,m})/\alpha
\end{aligned}
$$

Then

$$
\begin{aligned}
S_{i,k} &= 2\sigma_k Q_{3,i} - 4Q_{2,i} + \sigma_k^2 R_{3,i} - 4\sigma_k R_{2,i} + 2R_{1,i} \\
\mathbf{S}_{i,k} &= Q_{1,i} + \sigma_k R_{1,i}, \quad i = 1,2,\ldots 9 \\
T_{i,k} &= -2\sigma_k^3 P_{4,i} + 14\sigma_k^2 P_{3,i} - 20\sigma_k P_{2,i} + 4P_{i,1} \\
\mathbf{T}_{i,k} &= -2\sigma_k^2 P_{2,i} + 4\sigma_k P_{1,i}, \quad i = 1,2,3
\end{aligned}
$$

References

[1] Hall, M. G., "The Structure of Concentrated Vortex Cores," *Progress in Aeronautical Sciences*, edited by D. Küchemann, Vol. 7, Pergamon Press, Oxford, 1966, pp. 53–110.

[2] Bossel, H. H., "Vortex Breakdown Flowfield," *The Physics of Fluids*, Vol. 12, No. 3, March 1969, pp. 498–508.

[3] Bossel, H. H., "Inviscid and Viscous Models of the Vortex Breakdown Phenomenon," Rept. AS-67-14, 1967, College of Engineering, Univ. of California, Berkeley, Calif.

[4] Gartshore, I. S., "Some Numerical Solutions for the Viscous Core of an Irrotational Vortex, Aero. Rept. LR-378, 1963, National Research Council, Canada.

[5] Hall, M. G., "A Numerical Method for Solving the Equations for a Vortex Core," RAE TR 65106, 1965, Royal Aircraft Establishment, Farnborough, England.

[6] Mager, A., "Incompressible, Viscous, Swirling Flow Through a Nozzle," AIAA Paper 70–51, New York, 1970.

[7] Bossel, H. H., "Use of Exponentials in the Integral Solution of the Parabolic Equations of Boundary Layer, Wake, Jet, and Vortex Flows," *Journal of Computational Physics*, Vol. 5, No. 3, June 1970, pp. 359–382.

[8] Dorodnitsyn, A. A., "General Method of Integral Relations and its Application to Boundary Layer Theory," *Advances in Aeronautical Sciences*, Vol. 3, Pergamon Press, New York, 1962, pp. 207–219.

[9] Bethel, H. E., "Approximate Solution of the Laminar Boundary-Layer Equations with Mass Transfer," *AIAA Journal*, Vol. 6, No. 2, Feb. 1968, pp. 220–225.

[10] Bossel, H. H., "Boundary Layer Computation by an N-Parameter Integral Method Using Exponentials," *AIAA Journal*, Vol. 8, No. 10, Oct. 1970, pp. 1841–1845.

[11] Mitra, N. K., "Application of the Method of Weighted Residuals in the Computation of Laminar Compressible Boundary Layers," Ph.D. thesis, Oct. 1970, Mechanical Engineering Dept., Univ. of California, Santa Barbara, Calif.; available through University Microfilms, Ann Arbor, Mich.

[12] Fraenkel, L. E., "On the Flow of Rotating Fluid Past Bodies in a Pipe," *Proceedings of the Royal Society*, Vol. A233, 1956, pp. 506–526.

[13] Bossel, H. H., "Stagnation Criterion for Vortex Flows," *AIAA Journal*, Vol. 6, No. 6, June 1968, pp. 1192–1193.

[14] Hall, M. G., "On the Occurrence and Identification of Vortex Breakdown," RAE TR 66283, 1966, Royal Aircraft Establishment, Farnborough, England.

[15] Burgers, J. M., "Application of a Model System to Illustrate Some Points of the Statistical Theory of Free Turbulence," *Proceedings of the Academy of Sciences*, Amsterdam, Vol. 43, No. 1, 1940, pp. 2–12.

[16] Hummel, D., "Untersuchungen über das Aufplatzen der Wirbel an schlanken Deltaflügeln," *Zeitschrift für Flugwissenschaften*, Vol. 13, No. 5, May 1965, pp. 158–168.

[17] Hall, M. G., "A Theory for the Core of a Leading Edge Vortex," *Journal of Fluid Mechanics*, Vol. 11, Pt. 2, Sept. 1961, pp. 209–228.

[18] McCormick, B. W., Tangler, J. L., and Sherrieb, H. E., "Structure of Trailing Vortices," *Journal of Aircraft*, Vol. 5, No. 3, May–June 1968, pp. 260–267.

[19] Batchelor, G. K., "Axial Flow in Trailing Line Vortices," *Journal of Fluid Mechanics*, Vol. 20, Pt. 4, Dec. 1964, pp. 645–658.

[20] Lambourne, N. C. and Bryer, D. W., "The Bursting of Leading-Edge Vortices—Some Observations and Discussion of the Phenomenon," ARC R and M No. 3282, April 1961, Aeronautical Research Council, Britain.

[21] Harvey, J. K., "Some Observations of the Vortex Breakdown Phenomenon," *Journal of Fluid Mechanics*, Vol. 14, Pt. 4, Dec. 1962, pp. 585–592.

[22] Benjamin, T. B., "Some Developments in the Theory of Vortex Breakdown," *Journal of Fluid Mechanics*, Vol. 28, Pt. 1, April 1967, pp. 65–84.